DOI: 10.1002/adma.200800742

Scanning Photoemission Microscopy of Graphene Sheets on SiO_2**

By *Ki-jeong Kim, Hangil Lee, Jae-Hyun Choi, Young-Sang Youn, Junghun Choi, Hankoo Lee, Tai-Hee Kang, M. C. Jung, H. J. Shin, Hu-Jong Lee, Sehun Kim,** and *Bongsoo Kim**

Since Geim and his coworkers[1] succeeded in extracting individual sheets of carbon atoms (graphene) from graphite crystals, graphene has been attracted much attention for its scientific and technological importance.[2,3] Moreover, its peculiar electronic properties can be modified by changing the layer thickness and by controlling the carrier density using metals or molecules.[4–6] In addition, the modification of graphene surfaces using a direct chemical grafting process[7] has also become an important means of further expanding their potential.

In general, a graphene layer is prepared in ambient environments on SiO_2, and graphene devices are typically fabricated by using electron lithography as graphene is exposed to photoresist. These treatments in the lithography process can leave many adsorbates on the graphene surface, which may modify the electronic transport properties and play a role in reported graphene response to gas exposure. Therefore, it is important to interpret the transport properties correctly by considering the experimental variables such as the substrate effect and the presence of impurities. Especially, the strength of the interaction between the underlying substrate and the graphene film is an important issue in the study of monolayers of these materials. However, no direct chemical analysis using core level photoemission spectroscopy (CLPES) has been reported.

Ohta et al.[4] reported that interactions between a graphene film and a SiC substrate are weak by using angle-resolved ultraviolet photoemission spectroscopy (ARUPS). On the other hand, a scanning tunneling microscopy (STM) study reported that the observed graphene structures are significantly affected by the interaction between the graphite layer and the underlying substrate.[3,8] Moreover, STM topographic images[9,10] on a single layer of graphene on SiO_2 show the full, hexagonally symmetric honeycomb structure expected for an ideal, unperturbed graphene crystal. However, STM images obtained for multilayer graphene films on SiO_2 display a reduced, three-fold symmetry that is characteristic of the surface of bulk graphite crystals. In addition, theoretical calculations of the electronic structure and the minimum conductance of a graphene layer on SiO_2 using density functional methods show that there is a local variation of the Fermi energy of the graphene sheet attributed to the graphene/substrate interaction.[11]

In this Communication, we present a scanning photoemission microscopy (SPEM) study of graphene flakes on SiO_2. SPEM is a powerful tool for investigating the chemical information of the local area of the surface. By combining spatially resolved elemental and chemical mapping with sub-micrometer spot photoemission spectroscopy, SPEM can provide quantitative and qualitative information with high lateral and energy resolution.[12,13] Here, we were able to measure a piece of local information instead of average information, and distinguish a single-layer from a multilayer by using SPEM with a microfocused beam. We are interested in whether or not there is any difference between the monolayer graphene and the multilayer graphene in the C 1s core-level spectra and if it is possible to determine the layer thickness using the differences. Developing a method for measuring the material thickness is of particular importance because the thickness is a key structural factor determining the characteristics of graphene-based devices. To the best of our knowledge, this is the first demonstration of the systematic microscopic images for graphene sheets using SPEM.

Figure 1a shows an optical image of graphene flakes on SiO_2. According to the optical density examined in this study and also by atomic force microscopy (AFM), we were able to identify the thickness of the graphene layers. With this tool, we

[*] Dr. B. Kim, K.-j Kim, H. Lee, M.-C. Jung, T.-H. Kang, H. J. Shin
Pohang Accelerator Laboratory
POSTECH, Pohang
Kyungbuk 790-784 (Korea)
E-mail: kbs007@postech.ac.kr
K.-j. Kim, Y. S. Youn, J. Choi, Prof. S. Kim
Department of Chemistry and
School of Molecular Science (BK21)
KAIST
Daejeon 305-701 (Korea)
E-mail: sehun-kim@kaist.ac.kr
J.-H. Choi, H. Lee, H.-J. Lee, Dr. B. Kim
Department of Physics
POSTECH, Pohang
Kyungbuk 790-784 (Korea)

[**] This work was supported by the Nuclear R&D programs funded by the Ministry of Science and Technology (MOST) of Korea (grant no. MOST-2007-01156), the Center of Fusion Technology for Security, the SRC program (Center for Nanotubes and Nanostructured Composites) of MOST/KOSEF (grant no. R11-2001-00002-0), Brain Korea 21 Project (KRF-2006-312-C00565) the national R&D Projects for Nano Science and Technology Korea Research (grant no. KRF-2005-070-C00063), a Korea Research Foundation Grant funded by the Korean Government (MOEHRD) (KRF-2006-311-C00307), and the experiments at PLS were supported in part by MOST and POSTECH. One of the authors (H.L.) was supported by grant No R01-2006-000-11247 from the Basic Research Program of KOSEF.

 © 2008 WILEY-VCH Verlag GmbH & Co. KGaA, Weinheim WILEY InterScience® DISCOVER SOMETHING GREAT

ADVANCED MATERIALS

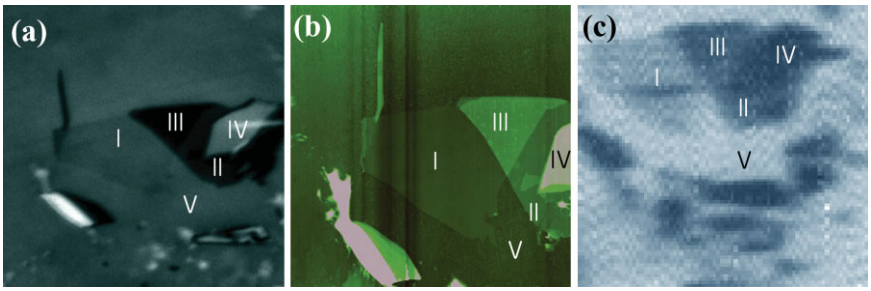

Figure 1. a) Optical image of a graphene flake consisting of mono- and multilayer graphene, b) AFM image, $20 \times 20\,\mu m^2$, c) SPEM image, $25 \times 25\,\mu m^2$. Region I, monolayer graphene; region II, double-layer graphene; region III, triple-layer graphene; region VI, multilayer graphene; region V, SiO_2 substrate.

could clearly identify five distinct regions: monolayer (I), double-layer (II), triple-layer (III), multilayer (IV), and SiO_2 (V) substrate. The white spotted features are the adhesive residues after the sample was fabricated. The thickness of each layer was also measured by AFM. Figure 1b is an AFM image of the graphene flake. We were able to determine the thickness of graphene more accurately using the AFM image. The multilayer structure at region IV has 15 layers. Figure 1c shows an SPEM image taken for the same graphene flake with 635 eV of incident photon energy. The SPEM image was obtained using a binding energy (BE) window between 288.2 and 281.8 eV of the C 1s core-level spectra. The intensity contrast in the maps indicates the amount of carbon on the composition of each thickness. Every region was identified in accordance with the layer thickness.

Through the simultaneously obtained 16 SPEM images with different BE windows (16 images with 0.4 eV energy separation), we were able to localize the mono-, triple-, and multilayered graphenes, because their electron yield distributions are different from each other, which will be discussed later.

Figure 2 displays a series of four images obtained from different BE windows, band width of 0.4 eV. Figure 2a shows an image that uses a centered BE of 285.2 eV. In this window, we could confirm that the bright region corresponds to monolayer graphene and the darkest region to multilayer graphene. With the same spectral analysis, we confirmed that Figure 2b–d shows images at the centered BE of 284.8, 284.4, and 284.0 eV, which reflect the enhanced brightness on the double-, triple- and multiple-layer graphene. The image measured at a BE of 284.8 eV in Figure 2b displays the double- and the triple-layer region with enhanced brightness. In Figure 2c, the monolayer graphene image disappears and the multiple-layer graphene image appears with enhanced brightness. The image taken at a BE of 284.0 eV in Figure 2b shows only multiple-layer graphene feature. These images signify that there are core-level-shifted features representing different chemical states depending on the layer thickness, measured from these images.

Figure 3 shows a series of C 1s spectra taken from imaged regions I, III, and IV. C 1s core level spectra of the mono- and multilayer graphene show significant changes in shape and intensities. For a more qualitative analysis, we introduced a fitting procedure. The C 1s spectra were decomposed with a Doniac and Sunjic[14] line shape, using a Lorentzian linewidth of 165 meV and an asymmetry parameter of 0.056.[15] The C 1s spectra were fitted with three components, as shown in Figure 3. The components with the higher BE, relative to that of bulk graphite (B), a BE of 284.2 eV with a core-level shift (CLS) of 1.67 eV (C), are known to originate from surface contaminants on SiO_2. The other component (with a CLS of 0.77 eV), denoted by S, is unknown yet. The peak, S, is a major peak on the monolayer graphene, and its intensity decreases as the graphene thickness increases. This peak is attributed to the interaction of the carbon of monolayer graphene with the SiO_2 substrate. Previous STM studies show a clear hexagonal structure for the monolayer graphene while three-fold structures appeared on a multilayer graphene. Also, Dharma-Wardana[11] have calculated the electronic structures and the minimum conductance of a graphene layer on SiO_2 using density functional methods, suggesting that when the Si–O substrate modifies the graphene bands, it could still lead to a spatially varying Fermi energy (E_F), with a variation of about $E_F \sim 0.6$ eV, and that the equilibrium separation between a large graphene sheet and the substrate would vary with the local substrate structure. Considering the report, peak S can be attributed to the C 1s that is interacting with the SiO_2

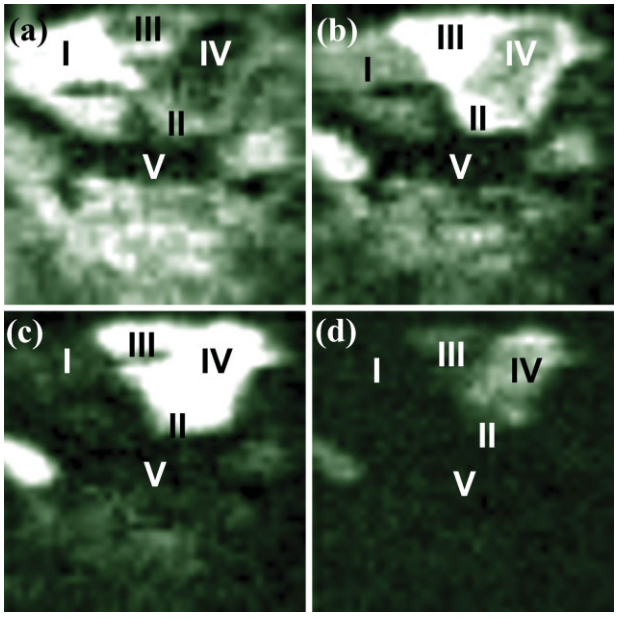

Figure 2. SPEM images simultaneously measured at different BE windows of a) 285.2, b) 284.8, c) 284.4, and d) 284 eV. The width of each window is 0.4 eV. It shows specific graphene layers with higher intensity depending on the specific BE window.

© 2008 WILEY-VCH Verlag GmbH & Co. KGaA, Weinheim

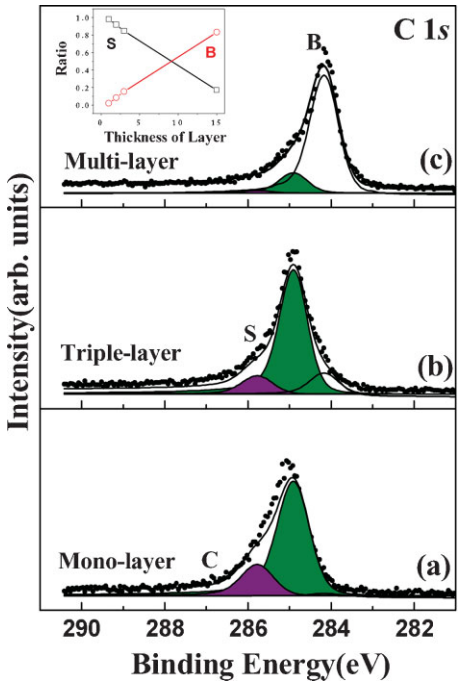

Figure 3. Photoemission spectra of C 1s core-level spectra measured on the local regions of I, III, and IV. These were measured at the photon energy of 635 eV (raw data (open circles), solid red lines (fitted data), monolayer components (gray areas), and multilayer components (hatched areas)). The inset shows an area ratio of monolayer component S (open squares) and multilayer component B (open circles) depending on the layer thickness.

substrate, and peak B to the bulk carbon in graphite configuration. The inset of Figure 3 shows the area ratio of S and B components with respect to the summation area of S and B as a function of the layer thickness. As shown in this figure, it shows good linearity with the layer thickness. Recently, Raman spectroscopy proved to be a reliable, nondestructive tool for the identification of mono- and multilayer samples.[16] Our result implies that measuring the ratio of the components S and B of the C 1s core-level spectra can be applied to estimate the layer thickness.

In conclusion, we measured the SPEM images of a graphene flake under ultrahigh vacuum conditions, and can distinguish a single-layer graphene from a multilayer graphene though the chemical contrast image of SPEM. There is a core-level shift on the monolayer graphene that originates from graphene–substrate interaction. The area ratios of S and B peaks of C 1s core-level spectra may also be utilized to determine the thickness of graphene sheets.

Experimental

The graphene films used in this study were prepared by mechanically exfoliating bulk natural graphite (POSCO, Korea) following the procedure reported by Geim and co-workers [1]. The peeled-off graphitic flakes were deposited on the surface of a silicon wafer covered with a 300 nm thick silicon dioxide film. Graphene flakes of monolayer thickness were initially selected from a vast majority of thicker flakes by visual inspection on an optical microscope. Through AFM, we measured the step height. The synchrotron radiation SPEM measurements were performed at the 8A1 beamline of the Pohang Accelerator Laboratory in Korea. The C 1s core-level spectra were measured with an incident angle of 0° and an emission angle of 55°, where the angle is 0° when the directions are perpendicular to the surface. The incident-photon beam size on the sample was 1 μm.

Received: March 17, 2008
Revised: April 10, 2008
Published online:

[1] K. S. Novoselov, A. K. Geim, S. V. Moozov, D. Jiabg, Y. Zang, S. V. Dovonos, I. V. Gregoriva, A. A. Firsov, *Science* **2004**, *306*, 666.
[2] A. K. Geim, K. S. Novoselov, *Nat. Mater.* **2007**, *6*, 183.
[3] C. Berger, Z. Song, X. Li, X. Wu, N. Brown, C. Naud, D. Mayou, T. Li, J. Hass, A. N. Marchenkov, E. H. Conrad, Ph. N. First, W. A. de Heer, *Science* **2006**, *312*, 1191.
[4] T. Ohta, A. Bostwick, T. Seyller, K. Horn, E. Rotenberg, *Science* **2006**, *313*, 951.
[5] E. H. Hwang, S. Adam, S. Das Sarma, *Phys. Rev. B* **2007**, *76*, 195421.
[6] H. B. Heersch, P. J. Herrero, J. B. Oostinga, L. M. Vandersypen, A. F. Morpurgo, *Nature* **2007**, *446*, 56.
[7] M. Delamar, R. Hitmi, J. Pinson, J. M. Saveant, *J. Am. Chem. Soc.* **1992**, *114*, 5883.
[8] T. A. Land, T. Michely, R. J. Behm, J. C. Hemminger, G. Comsa, *Surf. Sci.* **1992**, *264*, 261.
[9] E. Stolyarova, K. T. Rim, S. Ryu, J. Maultzsch, P. Kim, L. E. Brus, T. F. Heinz, M. S. Hybertsen, G. W. Flynn, *Proc. Natl. Acad. Sci. USA* **2007**, *104*, 9209.
[10] N. Ishigami, J. H. Chen, W. G. Cullen, M. S. Futher, E. D. Williams, *Nano Lett.* **2007**, *7*, 1643.
[11] M. W. C. Dharma-wardana, *J. Phys.: Condens. Matter* **2007**, *19*, 386228.
[12] M. P. Kiskinova, *Int. J. Image Syst. Tech.* **1997**, *8*, 462.
[13] H. J. Shin, M. K. Lee, *Appl. Phys. Lett.* **2001**, *79*, 1057.
[14] S. Doniach, M. Sunjic, *J. Phys. C* **1970**, *3*, 285.
[15] K. C. Prince, I. Ulrych, M. Peloi, B. Ressel, *Phys. Rev. B* **2000**, *62*, 6866.
[16] A. C. Ferrari, J. C. Meyer, V. Scardaci, C. Casiraghi, M. Lazzeri, F. Mauri, S. Piscanec, D. Jiang, K. S. Novoselov, S. Roth, A. K. Geim, *Phys. Rev. Lett.* **2006**, *97*, 187401.

© 2008 WILEY-VCH Verlag GmbH & Co. KGaA, Weinheim